BIOSYSTEMS ENGINEERING 156 (2017) 96–107

Available online at www.sciencedirect.com

ScienceDirect

journal homepage: www.elsevier.com/locate/issn/15375110

Research Paper

Developing and evaluating a finite element model for predicting the two-posts rollover protective structure nonlinear behaviour using SAE J2194 static test

Farzaneh Khorsandi [a,*], *Paul D. Ayers* [a], *Timothy J. Truster* [b]

[a] *Department of Biosystems Engineering and Soil Science, University of Tennessee, Knoxville, TN, USA*
[b] *Department of Civil & Environmental Engineering, University of Tennessee, Knoxville, TN, USA*

ARTICLE INFO

Article history:
Received 2 August 2016
Accepted 24 January 2017
Published online 13 February 2017

Keywords:
Finite element analysis
ROPS
Standard test
Virtual test

This research focuses on applying Non-linear Finite Element (FE) techniques to predict ROPS force-deflection curves under the simulated standardised static tests. The Society of Automotive Engineers (SAE) J2194 ROPS static standard test was selected for this study. According to the SAE J2194 standard, ROPS must be capable of absorbing predefined levels of energy under longitudinal (rear) and transverse (side) load tests before collapsing as well as avoiding large deformations that infringe upon the driver's clearance zone or leave the clearance zone unprotected. A nonlinear finite element approach was used to predict the response of two rear-mount two-post ROPS under simulated side and rear test conditions for Allis Chalmers 5040 and Long 460 tractors. The ROPS were designed with the Computer-based ROPS Design Program using a bolted corner bracket assembly to simplify the ROPS design process. The recommended FE model (ASTM, C3D10M, 0.01) was found to predict the ROPS performance deflection (RPD) with average error less than 10% compared to experimental test measurements. The FE model predicted the ROPS behaviour under rear loads more accurately than under side loads. The developed FE model based on measured stress–strain curves from test specimens was found to predict the ROPS behaviour more accurately than the FE models developed based on the Ramberg–Osgood material model.

1. Introduction and literature review

The agriculture industry has been ranked among the most dangerous industries in the United States. The US Bureau of Labour reported that approximately 123 farmers and farm workers died from work-related injuries in the USA in 2013 (Bureau of Labor Statistics, 2014). Tractor accidents are the leading cause of mortality in agriculture, accounting for one-half of all fatal agricultural accidents (Hoy, 2009). Tractor overturning is the main cause of mortality in tractor accidents (Springfeldt, 1996), which includes tipping the tractor sideways or backward (Ayers, Dickson, & Warner, 1994). Tractor rollover accounts for up to one-third of all tractor-related fatalities

* *Corresponding author*. 2506 E. J. Chapman Drive, Knoxville, TN 37996, USA.
E-mail address: fkhorsan@vols.utk.edu (F. Khorsandi).
http://dx.doi.org/10.1016/j.biosystemseng.2017.01.010

Nomenclature

Symbol

E	Modulus of elasticity, Pa
E_n	Absorbed energy, J
M	Tractor reference mass, kg
q	Material hardening index, –
ε_x	Axial strain, –
σ_u	Ultimate stress, Pa
σ_y	Yield stress, Pa
υ	Poisson's ratio, –

Abbreviations

C3D10M	Continuum three-dimensional with ten nodes modified
C3D4	Continuum three-dimensional with four nodes
CRDP	Computer based ROPS Design Program
FE	Finite element
RAD	ROPS Allowable Deflection
ROPS	Roll-Over Protective Structure
RPD	ROPS Performance Deflection

(Murphy & Yoder, 1998). The use of a Rollover Protective Structure (ROPS) in a combination with a seat belt has proven to be the most effective method to prevent fatalities from tractor overturning. A ROPS is a frame or cab which is installed on the tractor to protect the operator by absorbing a portion of the impact energy generated by the tractor weight in a rollover accident. The ROPS provides a safe zone, called the clearance zone, between the envelope of the ROPS and tractor seat. Of the several types of ROPS such as two-post ROPS, four-post ROPS, and cab, the most common is the two-post ROPS (Murphy & Buckmaster, 2014), which consists of a reversed U-shaped crossbar located above the head of the operator on posts which are bolted to the vehicle frame or axle housing.

1.1. *Roll-Over Protective Structure performances and regulations*

The first standard for evaluating ROPS performance was developed in Sweden in the 1950s (OEEC, 1959). The use of standard ROPS on tractors in Sweden was a significant factor in decreasing the number of fatal rollover accidents from 15 in 1957 to only one fatality in 1990 (Thelin, 1998). In the United States (US), the Occupational Safety and Health Administration (OSHA) required almost all tractors produced after 1976 and operated by nonfamily employees on US farms to be equipped with ROPS. Only 10% of the farm tractors in the US fall under the OSHA jurisdiction (Reynolds & Groves, 2000). Increasingly since 1985, about 59% of the tractors produced by manufacturers in the US are equipped with ROPS (Ayers et al., 1994; CDC, 2014). However, tractor rollover is still a common type of fatal accident in the US, and a significant amount of tractors are still not equipped with standardised ROPS.

Several ROPS design programs have been developed in recent years such as CRDP and ESTREMA (Ayers, Khorsandi, John, & Whitaker, 2016; Mangado et al., 2007). The ESTREMA program was developed to facilitate ROPS design calculations. A ROPS for Massey Ferguson model 178 tractor was designed with ESTREMA. The designed ROPS has a satisfactory performance under the OECD code 4 (OECD, 2012). The performance of the designed ROPS with these ROPS design programs needs to be examined in advance.

The ROPS performance must be determined through applicable standard tests. The SAE (2009) static test is a low demanding test in which the data collection is straightforward and the results are reliable and accurate (Ross & DiMartino, 1982). Most manufacturers select the static test for ROPS evaluation (Fabbri & Ward, 2002). The static test for rigid two-post ROPS includes a sequence of four static loads: (1) horizontal rear (longitudinal), (2) first vertical, (3) horizontal side (transverse), and (4) second vertical loadings. The displacement rate in the horizontal static test must be less than 5 mm s^{-1}. The ROPS passes the static test if it absorbs a predefined level of energy in longitudinal and transverse tests and tolerates a particular force in the vertical test without structural member rupture. Also, the ROPS should not infringe the clearance zone (intrusion criteria), and the ROPS should not leave clearance zone unprotected from the ground plane (exposure criteria). The ROPS rupture is indicated by incapability to tolerate additional loading.

Designing ROPS to pass the appropriate standard is a challenge for manufacturers, which increases ROPS production expenses. ROPS design requires a balance of 1) ROPS material strength and allowable deflection to meet energy criteria, 2) elastoplastic material properties to decrease peak moments at the mounting brackets, and 3) ROPS positioning and alignment to provide a safe zone for the operator. Excessively rigidity transmits a significant shock to the mounting and exerts a considerable force and moment to the chassis. Overly flexible structures deform substantially under the load and infringe on the safe zone or leave the clearance zone unprotected.

1.2. *Modelling*

While the static test is less demanding than the alternative dynamic or field-upset test, it is still costly and time-consuming. The ROPS deformation during the static test can be evaluated more accurately compared to the dynamic test (Chisholm, 1979), therefore the static test is more effective in ROPS design improvement. Fabbri and Ward (2002) reported that about one-third of ROPS standard tests failed at the Bologna test stations in Italy. The test failure prolongs the ROPS production and increases the project expenses. Using the experimental performance test alone does not provide an efficient ROPS design process. Therefore, researchers have used a combination of experimental tests and mathematical models to improve and evaluate ROPS performance (Chen, Wang, Zhang, Zhang, & Si, 2012; Karliński, Rusiński, & Smolnicki, 2008). The ROPS experimental tests have not been replaced with mathematical models, since SAE (2009) does not allow theoretical model results to satisfy the ROPS performance test. Nonetheless, modelling increases the understanding of the ROPS behaviour under the standardised

test and can be used as a tool to evaluate minor structural modifications and also decrease the possibility of test failure.

Several authors developed analytical models for predicting the behaviour of ROPS in simulated standardised tests (Clark, 2005; Kim & Reid, 2001; Swan, 1988; Thambiratnam, Clark, & Perera, 2009; Yeh, Huang, & Johnson, 1976). Subsequently, numerical approaches such as the finite element (FE) method have been applied to simulate ROPS deflection under the standard tests.

Fabbri and Ward (2002) developed an FE-based program to predict common ROPS behaviour under the Organization for the Economic Co-operation and Development (OECD, 2008) and the Economic European Community (EEC, 1987) standardised tests. The developed FE model employed several different material models such as elastic-perfectly plastic, bi-linear, tri-linear or the Ramberg–Osgood model. The FE model results were compared with the results of the experimental test, analytical and numerical models developed with commercial software packages. The developed FE model was accurate for predicting force-deflection to within 30% percent of the actual test values of a two-post ROPS with stiff fixing points to the tractor. In the case of weak fixing points, the FE model results were within 50% of the actual test values. The developed program was able to predict the behaviour of cabs and four-post ROPS with errors less than 20%. The accuracy of the program was directly related to the accuracy of the geometry creation, the description of the material properties, and the boundary conditions.

Alfaro, Arana, Arazuri, and Jarén (2010) simulated the standardised static test based on the OECD code 4 and SAE J2194 using Abaqus commercial FE package. The FE model predictions for a four-post ROPS and a cab indicated close agreement with experimental test data. They estimate the maximum allowable tractor mass based on the ROPS force-deflection curves under the simulated standardised test. Harris, Winn, Ayers, and McKenzie (2011) developed an FE model utilising a bi-linear stress–strain relationship in ANSYS to predict cost-effective ROPS performance under the SAE J2194 and OSHA 29 CFR 1928.52 standard tests. After calibration, the FE model could predict the force for rear load and side load with an accuracy of 10% and 5%, respectively, at the point when the ROPS met the energy criterion. The authors conclude that the SAE J2194 static test provides a more conservative design test than the OSHA static test.

1.3. *Justification*

The experimental standardised ROPS tests are expensive, laborious, time-consuming, and destructive. About one-third of ROPS fail the standard tests, and the test failure postpones ROPS production project and increases the project expenses. Using the experimental test alone is inefficient in improving the ROPS design and performance. Modelling has been introduced as a method that can simulate the ROPS performance in standard tests, speeds up the design process, evaluates ROPS modifications, and reduces the ROPS production expenses. Although computer models can predict the force-deflection curve of ROPS, the experiment test cannot be replaced with computer models. The modelling approach is needed to increase the possibility that the designed ROPS is likely to pass the standard before the experimental test. Therefore researchers have used a combination of experimental tests and mathematical models to improve and test ROPS performance.

There is no FE model available to predict the behaviour of rear-mount two-post ROPS designed by newly developed Computer-based ROPS Design Program (CRDP). CRDP is a computer program for ROPS design based on tractor dimensions and weight (Ayers et al., 2016). In this study, two ROPS for two models of tractor were designed using CRDP. The designed ROPS using the CRDP are assembled mainly using bolts. The bolted corner bracket attachment at the corners may rotate and absorb some of the energy during the loading test, especially side load test. There is also some adjustment at bolts holes which affects the ROPS deflection.

In some of the previous FE models, the model needed to be calibrated to predict the ROPS behaviour (Alfaro et al., 2010; Thambiratnam et al., 2009). The material properties and stress–strain behaviour are critical inputs of the FE model. None of the founded FE models have reported using experimentally measured constitutive relations in the plastic region for ROPS. In the previous studies constitutive laws such as Ramberg–Osgood, elastic-perfectly plastic, bi-linear, and tri-linear were used (Fabbri & Ward, 2002; Harris et al., 2011; Thambiratnam et al., 2009).

1.4. *Objective*

In this work, an FE model with no calibration was developed to predict the performance of agricultural tractors ROPS designed by CRDP, under the static SAE J2194 standard. The specific objectives comprised 1) simulating the SAE J2194 static side and rear loading tests for ROPS, 2) predicting the force-deflection results of the ROPS under simulated standard tests, 3) comparing the ROPS performance deflection (RPD) for the simulated and experimental tests, and 4) evaluating the influence of elastic plastic material properties of the ROPS on simulation results.

2. Material and methods

The FE model was developed in three steps: 1) design and manufacture the ROPS, 2) examine the ROPS performance under the experimental test, and 3) develop and validate the FE model. Two ROPS for Allis Chalmers 5040 and Long 460 tractors were designed using CRDP (Ayers et al., 2016). The behaviour of the designed ROPS were evaluated experimentally based on SAE J2194 standard test. The FE model was developed using Abaqus (version 6.11–1, 2011. ABAQUS Inc., Providence, RI, USA) and validated by comparing the predicted and experimental test results with four different tests, side and rear load tests for Allis Chalmers 5040 and Long 460 ROPS.

The tests are destructive, as both elastic and plastic deflections take place during the test, therefore it is impossible to replicate the tests for a single ROPS. The model was validated with four different tests (side and rear load tests for Allis Chalmers 5040 and Long 460 ROPS). These four validations cannot be considered “replications”, but considered together can be used to evaluate the validity of FE model results.

2.1. *Design the Roll-Over Protective Structure with Computer based ROPS Design Program*

CRDP was developed to generate ROPS designs based on 46 tractor dimensions and the tractor weight (Ayers et al., 2016). The program outputs were the two-post, rear-mount ROPS drawings which can be used to construct the ROPS (Fig. 1). The drawing includes the posts, crossbeam, baseplate, corner brackets, and strappings. All of the ROPS dimensions were presented in the CAD drawing within a Microsoft Excel file. The parts were assembled using bolts to secure the corner brackets and welding for the strapping and baseplate attachment. The final drawing is presented in Fig. 1. The constructed ROPS using the CRPD needs to be tested based on standardised experimental tests (Ayers et al., 2016).

The summaries of Allis Chalmers 5040 and Long 460 ROPS dimensions are presented in Tables 1 and 2. The manufacturing tolerances for plates were 1 mm and for posts and cross beams were 5 mm. The tolerances for width, length and thickness of the tubes were 0.8, 0.6, and 0.5 mm, respectively. The plate tolerances for corner brace is 1.14 mm and for top and bottom base plates are 1.52 mm. These two models of tractors were selected because there is no commercially available ROPS for them and they are among the most frequently requested ROPS from the New York Centre for Agricultural Medicine and Health ROPS retrofit program (Ayers et al., 2016)

2.2. *Experimental test*

The constructed ROPS were sent to FEMCO Inc. in McPherson, KS, for experimental static standard tests. The applied loads were regulated based on SAE (2009) standard tests. The test included sequences of rear and side tests. The test was conducted using a ROPS test stand, hydraulic cylinders, a data acquisition system, a force transducer, and a displacement potentiometer. The static tests were stopped when the energy criteria were met, and the ROPS deflections were recorded (Ayers et al., 2016).

The SAE (2009) standard test specifies that "the ROPS should be mounted on a tractor chassis or the equivalent for which ROPS is designed to assure the integrity of the entire system". The aim of this project was to examine the performance (deflection) of the designed ROPS under the standard test, not to evaluate the performance of entire structure. Therefore the ROPS was attached to the base directly with no chassis (Fig. 2).

2.2.1. *Longitudinal (rear) load test*

The rear load was applied horizontally and parallel to the longitudinal tractor median plane. Since more than half of the tractors weight was on the rear wheels, the longitudinal loads were applied from the rear. The load was applied to the cross beam, typically the first component that contacts the ground in a rear rollover accident (Fig. 2). The load was exerted to the cross beam and to the point which is located one-sixth of the cross bar width from one end of the cross beam. The rear load was applied until the ROPS absorbed energy (E_n) reached the required energy based on Eq. (1):

$$E_n = 1.4\,M \quad (1)$$

where E_n is the absorbed energy (J), and M is the tractor reference mass (kg). The absorbed energy is the area under the force-deflection curve.

2.2.2. *Transverse (side) loading*

The side load was inserted horizontally and perpendicular to the median longitudinal plane of the tractor. The side load pushed the one side of the cross beam at which the rear load

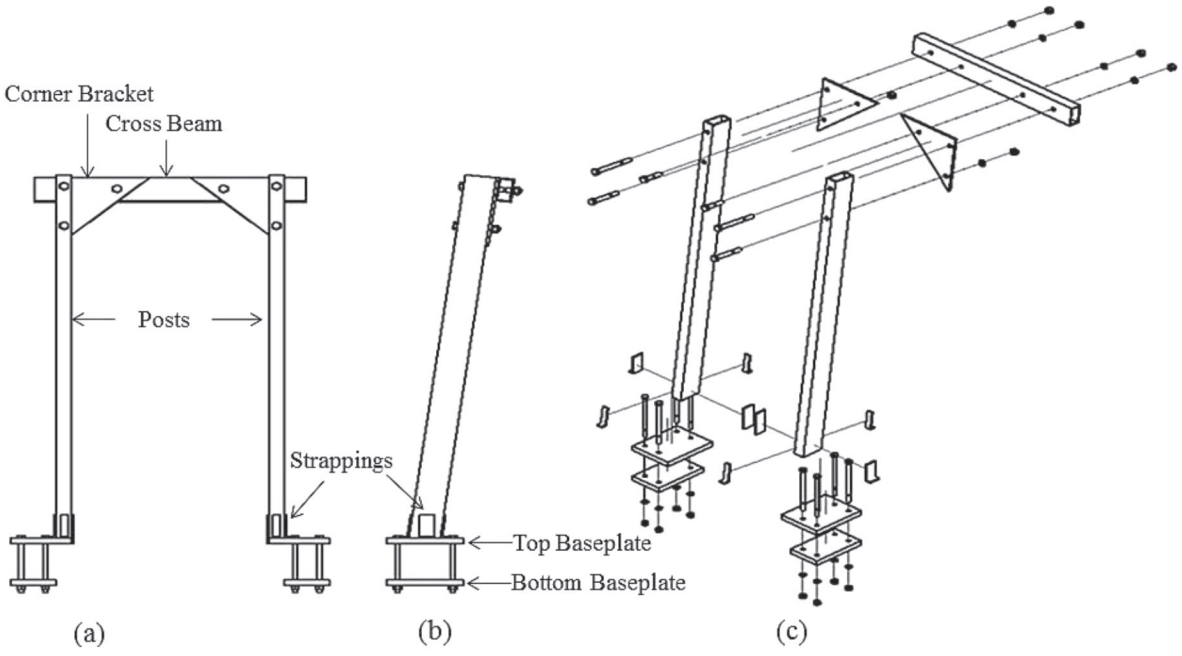

Fig. 1 – Drawing of the ROPS designed using CRDP (a) Front view. (b) Side view. (c) Exploded view (Ayers et al., 2016).

Table 1 – The output of CRDP. Summary of material and dimensions for Allis Chalmers 5040 ROPS (Ayers et al., 2016). All dimensions in mm.

Part	Quantity	Dimensions			
Posts tubing	2	Thickness = 4.8	Width = 50	Depth = 76	Length = 1772
Crossbeam tubing	1	Thickness = 4.8	Width = 76	Depth = 50	Length = 985
Top baseplate	2	Thickness = 19.1	Length = 225	Width = 159	
Bottom baseplate	2	Thickness = 19.1	Length = 225	Width = 147	
Corner braces	2	Thickness = 9.5	Length = 304	Width = 304	
Baseplate strapping	1	Thickness = 6.4	Length = 508	Width = 25	
Baseplate strapping	3	Thickness = 6.4	Length = 101	Width = 25	
Baseplate bolts	8	Diameter = 12.7	Grade = 8	Length = 254	

Table 2 – The output of CRDP. Summary of material and dimensions for Long 460 ROPS. All dimension in mm.

Part	Quantity	Dimensions			
Posts tubing	2	Thickness = 4.8	Width = 50	Depth = 101	Length = 1610
Crossbeam tubing	1	Thickness = 4.8	Width = 101	Depth = 50	Length = 642
Top baseplate	2	Thickness = 25.4	Length = 247	Width = 198	
Bottom baseplate	2	Thickness = 25.4	Length = 247	Width = 147	
Corner braces	2	Thickness = 9.5	Length = 304	Width = 304	
Baseplate strapping	3	Thickness = 6.4	Length = 101	Width = 25	
Baseplate strapping	1	Thickness = 6.4	Length = 127	Width = 50	
Baseplate bolts	8	Diameter = 15.9	Grade = 8	Length = 254	

Fig. 2 – Rear load test Long 460 ROPS.

had not been applied. The test stops when the absorbed energy is equal to:

$$E_n = 1.75\ M \quad (2)$$

2.2.3. *Performance parameters*

The reference mass and the required absorbed energies and loads for the Allis Chalmers 5040 and Long 460 tractors are presented in Table 3. The ROPS Allowable Deflection (RAD) is defined as the maximum allowable deflection of the ROPS without violating the intrusion or exposure criteria. The ROPS Performance Deflection (RPD) is defined as the ROPS deflection at the point that the ROPS absorbs the predefined levels of energy in horizontal tests and the ROPS deflection under the vertical tests. During all of the tests, the RPD must be smaller or equal to the RAD to satisfy SAE J2194 requirements.

Table 3 – Calculated applied force and required energy as a function of tractor mass based on SAE J2194 standard.

	Allis Chalmers 5040	Long 460
Tractor mass (kg)	2032	1842
Rear load test, required absorbed energy (J)	2845	2579
Rear load test, RPD (mm)	229	176
Rear load test, RAD (mm)	420	400
Rear load test, permanent deflection (mm)	96	70
Side load test, required absorbed energy (J)	3556	3224
Side load test, RPD (mm)	221	168
Side load test, RAD (mm)	295	30
Side load test, permanent deflection (mm)	108	87

A mathematical model was developed, validated, and implemented to evaluate the ROPS exposure criteria of ROPS under the standard SAE J2194 static test (Ayers et al., 1994). The model calculated RAD utilising tractor dimensions, ROPS mounting points, and ROPS dimensions. The RAD for Allis Chalmers 5040 and Long 460 ROPS were computed using a Matlab code which was based on Ayers et al. (1994) research (Table 3). The intrusion criteria were defined based on the ROPS dimensions and the location of ROPS mounting and clearance zone.

2.3. *Finite element model*

The ROPS behaviour under standard tests were simulated by developing 24 FE models in Abaqus (version 6.11–1). Abaqus was selected for this study because it is one of the most robust commercial software packages for nonlinear analysis (Yu & Li, 2012). The overall modelling procedure in FE software packages includes six steps to investigate engineering problems such as predicting the nonlinear behaviour of ROPS: geometry

creation, defining material properties, mesh generation, determining boundary conditions, simulation execution, and post-processing.

The developed models included two types of ROPS (Long 460 and Allis Chalmers 5040), two finite element mesh resolutions and element types (C3D4 with global size 0.08, and C3D10M with global size 0.01), two tests (side and rear load test), and three material models 1) Experimental test based on ASTM test, 2) Ramberg–Osgood model based on ASTM test, and 3) Ramberg–Osgood model based on available online data).

The designed ROPS for this study were made of tubular elements with a rectangular cross section (Tables 1 and 2) which are reinforced with two bolted corner plates and welded strappings at the baseplates. The 3D CAD geometry model was drawn in 3D and was imported into Abaqus (Fig. 3).

2.3.1. *Material properties*

The material properties can have a significant influence on the FE results, and need to be evaluated. Typically, static ROPS testing produces a significant elastic–plastic deflection under SAE J2194 standard test; therefore material properties in both elastic and plastic ranges are required for the FE model. The tubular ROPS parts in this study were made of steel ASTM 500 grade B and the plates were made of steel ASTM A 513. Mechanical properties in the elastic range include modulus of elasticity (E) and Poisson's ratio (υ) (Table 4). The material property in the plastic range includes the stress–strain relationship which can be measured directly or predicted by applying material models. Three different constitutive relations for material in the plastic range were developed, including a stress–strain relationship developed based on the experimental test, and two constitutive relations developed based on Ramberg–Osgood model.

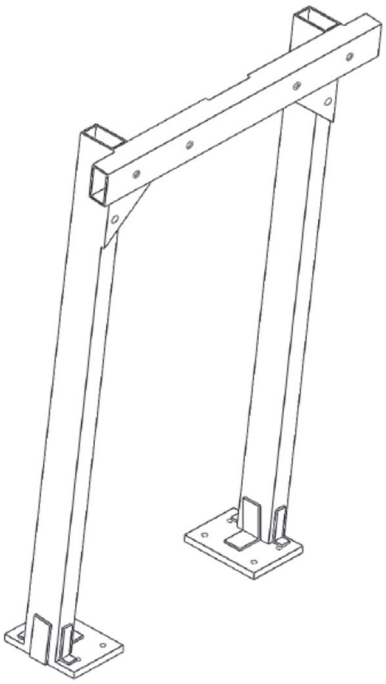

Fig. 3 – Creation of the ROPS geometry.

Table 4 – The measured material properties based on ASTM E8 standard.

Material properties	Source	
	(O'Neal steel, 2015)	ASTM results
Modulus of elasticity (MPa)	200	200
Poisson's ratio	0.33	0.33
Yield stress (MPa)	317.2	384.5
Ultimate stress (MPa)	399.9	494.3
Hardening index q	13.92	12.92

The tensile testing of ASTM steel 500 grade B was performed in accordance with ASTM E8 (E8/E8M-11, 2011). The specimen was removed from the sidewall of the steel tube used for manufacturing the ROPS. The material properties of the steel tube are assumed to be uniform throughout and equal to the specimen properties. The results include yield stress (σ_y), ultimate stress (σ_u), and the stress–strain relationship of steel (Fig. 4 and Table 4). The experimental tensile test is more expensive and time-consuming compared to using constitutive laws. Thus, the developed constitutive relations based on Ramberg–Osgood were used to predict the force-deflection curves (Eqs. (3) and (4)). This model can predict a stress–strain relationship based on values of E, σ_u, and σ_y which are usually available on-line for different steels. Several researchers have proved the accuracy of the Ramberg–Osgood model for predicting the elastic constitutive relations of steel alloys (Rasmussen, 2003; Wei & Elgindi, 2013).

$$\varepsilon(x) = \frac{1}{E}\sigma(x) + 0.002\left(\frac{1}{\sigma_y}\right)^{q-2}|\sigma(x)|^{q-2}\sigma(x) \tag{3}$$

$$q = 1 + \frac{\ln 20}{\ln(\sigma_u/\sigma_y)} \tag{4}$$

Both predicted and measured constitutive relations were used to develop different FE models and the final results were compared.

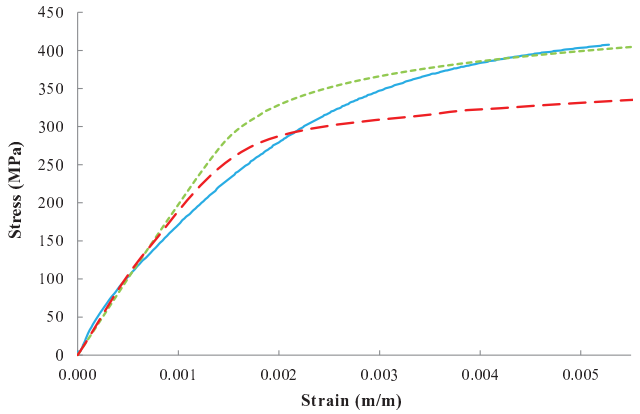

Fig. 4 – ASTM 500 steel grade B Stress–Strain relationships. Experimental ASTM E8 tests (—). Developed Ramberg–Osgood model based on experimental ASTM E8 data, $q = 12.92$ (– – –). Ramberg–Osgood model developed based on O'Neal steel, $q = 13.92$ (— —).

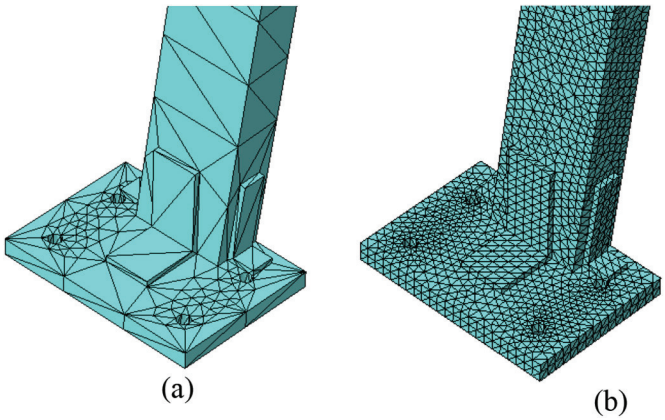

Fig. 5 – Basement plate of the Long 460 Meshed ROPS (a) C3D4 with global size 0.08 (b) C3D10M with global size 0.01.

2.3.2. *Mesh generation*

Two types of tetrahedral elements with two different element sizes were selected for meshing the ROPS, taking advantage of the automatic mesh generator. The ROPS were meshed using either four-node linear tetrahedral elements (C3D4) with global size 0.08 m or ten-node quadratic tetrahedral elements (C3D10M) with global size 0.01 m (Fig. 5). The global size means the average size of the elements, which are 0.08 m and 0.01 m respectively, because the SI unit (m) was used for this model. An element size of 0.01 m for the quadratic tetrahedral elements (C3D10M) was selected, as it resulted in minimum total error for all Allis Chalmers 5040 and Long 460 ROPS tests.

The tetrahedral elements provide a comprehensive description of geometrical details of problems which include both circular and rectangular parts. The second-order modified tetrahedral elements (C3D10M) are an effective alternative to the linear elements (C3D4), for complex geometries and are robust for large deformation. First order tetrahedral elements (C3D4) are usually overly stiff for force-displacement analysis and the convergence is slow with very fine mesh size (Ellobody, 2014).

2.3.3. *Determining the boundary condition*

Typically the ROPS are attached to the tractor chassis using bolts through baseplates. In this research, the fasteners between the ROPS and tractor was not modelled because US national institute for occupational safety and health reported that the deflection at this point is negligible (Harris, Mucino, Etherton, Snyder, & Means, 2000). Since the ROPS in the experimental tests were attached to a stiff fixed platform, the attachment points at the bottom of the baseplates were restrained in all six degrees of freedom within the FE model.

The forces were inserted based on the SAE J2194 standard as presented in Table 3. The side and rear loads were applied sequentially and as a pressure on a specific area and were increased at a constant rate from zero up to the point when the ROPS absorbs the predefined level of energy based on Eqs. (1) and (2). The ROPS has both elastic and plastic deflection. After each test, some residual plastic deflections remained in the ROPS that were considered in calculations by applying the loads sequentially.

Either load or displacement can be applied as the input for the FE model. The force-deflection curves were

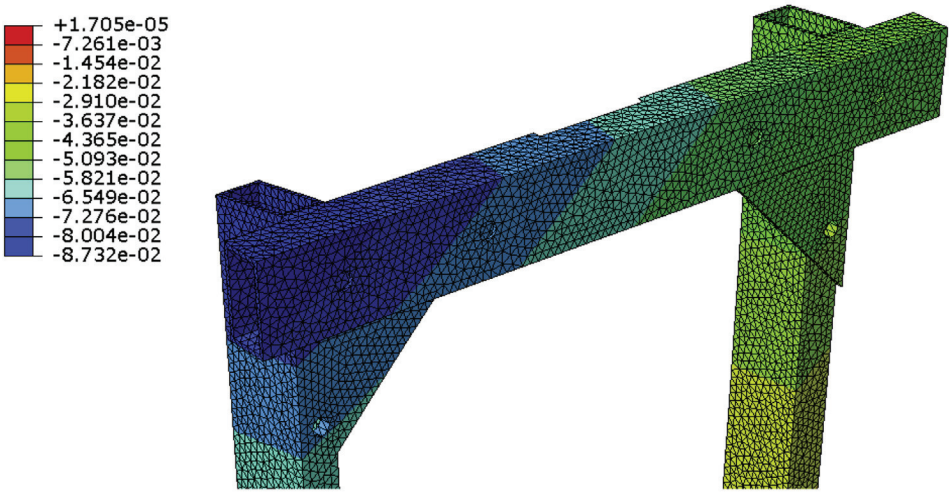

Fig. 6 – Rearward deflection (m) of the Long 460 ROPS under the rear load. The applied force was equal to 16 kN, the material constitutive relation was based on the experimental test (ASTM E8), mesh C3D10M, and mesh size 0.01.

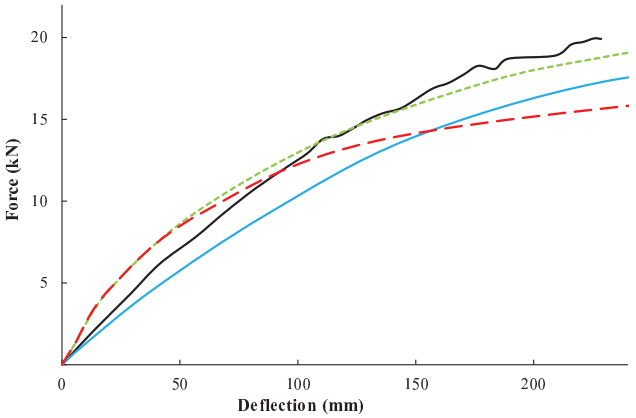

Fig. 7 – ROPS deflection under rear loading for Allis Chalmers 5040 ROPS (C3D10M, 0.01). Experimental test results (——). FE model results based on experimental ASTM E8 tests (——). FE model based on the developed Ramberg–Osgood model and experimental ASTM E8 data, $q = 12.92$ (– – –). FE model based on the Ramberg–Osgood model for O'Neal steel, $q = 13.92$ (— —).

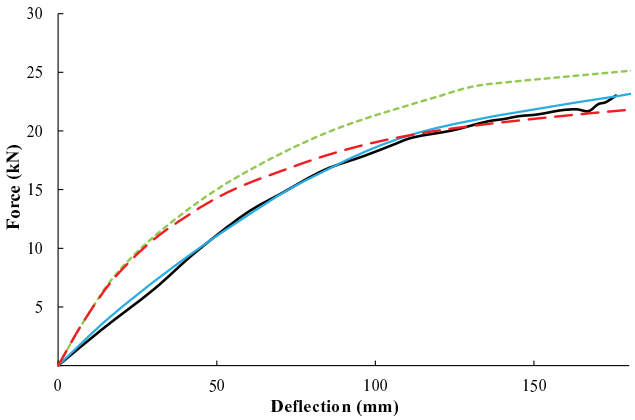

Fig. 9 – ROPS deflection under rear loading for Long 460 ROPS (C3D10M, 0.01). Experimental test results (——). FE model results based on experimental ASTM E8 tests (——). FE model based on the developed Ramberg–Osgood model and experimental ASTM E8 data, $q = 12.92$ (– – –). FE model based on the Ramberg–Osgood model for O'Neal steel, $q = 13.92$ (— —).

developed by applying either displacement or load. Results for each model were exactly the same. Because model development with load inputs is straightforward, this approach was taken. The loads were applied at intervals of one-tenth of the expected maximum required load. The loads were applied step-wise intervals of one-tenth of the expected maximum required load. The one-tenth interval was selected as the error of the calculated energy with this interval is sufficient for the required energy estimation. The load intervals ranged from 2000 to 3000 N. During each step, the deflections were calculated to develop the force-deflection curve.

3. Results and discussion

The results include the ROPS behaviour under the experimental and the simulated standard tests. The experimental test results for rear and side load test include the deflection, force, and absorbed energy. The experimental test results and FE model outputs were presented in two types of graphs, force-deflection and energy–deflection curves. The force-deflection curves were used to compute the energy–deflection curves.

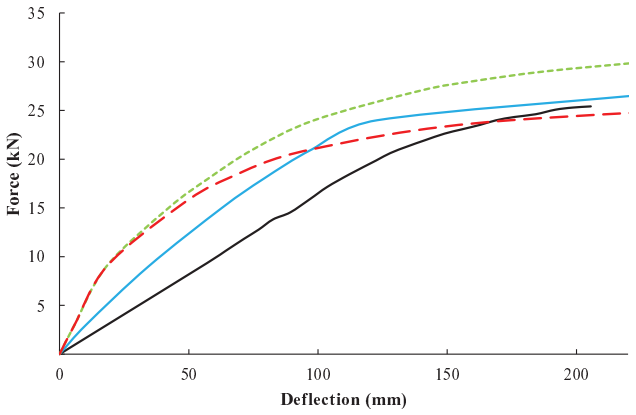

Fig. 8 – ROPS deflection under side loading Allis Chalmers 5040 ROPS (C3D10M, mesh size 0.01 m). Experimental test results (——). FE model results based on experimental ASTM E8 tests (——). FE model based on the developed Ramberg–Osgood model and experimental ASTM E8 data, $q = 12.92$ (– – –). FE model based on the Ramberg–Osgood model for O'Neal steel, $q = 13.92$ (— —).

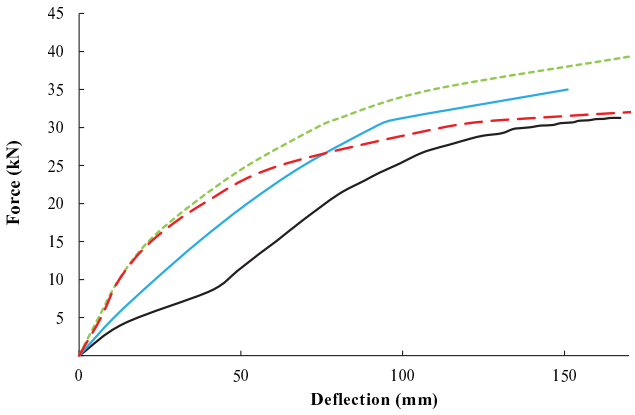

Fig. 10 – ROPS deflection under side loading Long 460 ROPS (C3D10M, 0.01). Experimental test results (——). FE model results based on experimental ASTM E8 tests (——). FE model based on the developed Ramberg–Osgood model and experimental ASTM E8 data, $q = 12.92$ (– – –). FE model based on the Ramberg–Osgood model for O'Neal steel, $q = 13.92$ (— —).

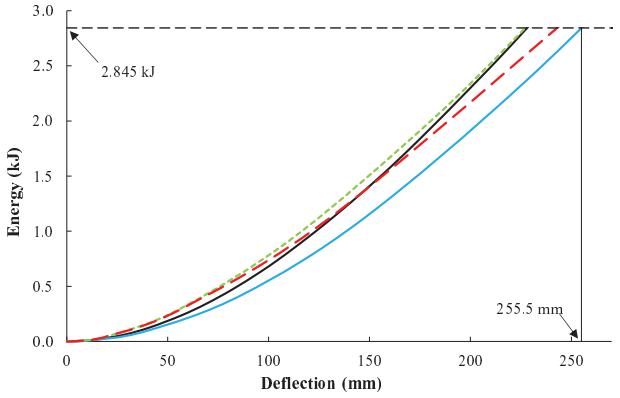

Fig. 11 – ROPS absorbed energy under rear loading for Allis Chalmers 5040 ROPS (C3D10M). Experimental test results (——). FE model results based on experimental ASTM E8 tests (——). FE model based on the developed Ramberg–Osgood model and experimental ASTM E8 data, $q = 12.92$ (– – –). FE model based on the Ramberg–Osgood model for O'Neal steel, $q = 13.92$ (— —). The required absorbed energy (– – –).

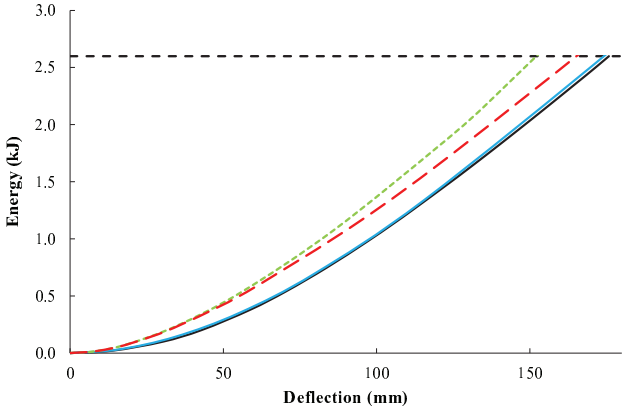

Fig. 13 – ROPS absorbed energy under rear loading for Long 460 ROPS (C3D10M). Experimental test results (——). FE model results based on experimental ASTM E8 tests (——). FE model based on the developed Ramberg–Osgood model and experimental ASTM E8 data, $q = 12.92$ (– – –). FE model based on the Ramberg–Osgood model for O'Neal steel, $q = 13.92$ (— —). The required absorbed energy (– – –).

The ROPS deflection under the applied load was calculated and used to develop the force-deflection curves. In Fig. 6, the deflection of Long 460 ROPS under the simulated rear load (16 kN) is shown. The deflection is equal to 0.0796 m at the measurement point which is the point at which ROPS deflection was measured in the experimental test.

The experimental and predicted force-deflection curves for rear and side load tests of the Allis Chalmers ROPS are presented in Figs. 7 and 8, respectively. Figures 9 and 10 show the force-deflection curves of the Long 460 ROPS under the experimental and simulated rear and side tests. The ultimate stress was checked based on Von Mises criterion and showed that there is no rupture in the structure during the tests (Figs. 7–10).

The effect of the steel properties on predicted force-deflection curves was examined. Three force-deflection curves were developed with Abaqus for each test by applying three levels of material properties including, one measured stress–strain relationship based on ASTM E8 and two predicted stress–strain curves based on Ramberg–Osgood model (Fig. 4). The material properties were measured experimentally, although in some of the previous models, constitutive laws were used (Fabbri & Ward, 2002;

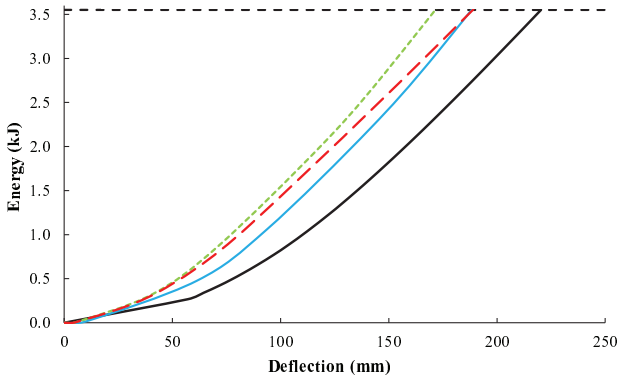

Fig. 12 – ROPS absorbed energy under side loading for Allis Chalmers 5040 ROPS (C3D10M). Experimental test results (——). FE model results based on experimental ASTM E8 tests (——). FE model based on the developed Ramberg–Osgood model and experimental ASTM E8 data, $q = 12.92$ (– – –). FE model based on the Ramberg–Osgood model for O'Neal steel, $q = 13.92$ (— —). The required absorbed energy (– – –).

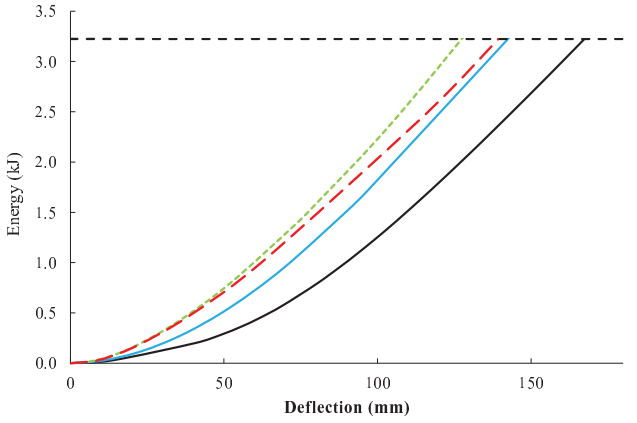

Fig. 14 – ROPS absorbed energy under side loading for Long 460 (C3D10M). Experimental test results (——). FE model results based on experimental ASTM E8 tests (——). FE model based on the developed Ramberg–Osgood model and experimental ASTM E8 data, $q = 12.92$ (– – –). FE model based on the Ramberg–Osgood model for O'Neal steel, $q = 13.92$ (— —). The required absorbed energy (– – –).

Table 5 – ROPS displacement at maximum absorbed energy (C3D10M).

	Allis Chalmers 5040 ROPS				Long 460 ROPS			
	Rear (mm)	Error (%)	Side (mm)	Error (%)	Rear (mm)	Error (%)	Side (mm)	Error (%)
RAD	426	–	295	–	400	–	360	–
Experimental	229	0.0%	221	0.0%	176	0.0%	168	0.0%
ASTM RPD	255.5	11.6%	196.0	−11.3%	174.0	−1.1%	144.0	−14.3%
RO O'Neal steel RPD	244.0	6.1%	193.0	−12.7%	166.0	−5.7%	128.0	−23.8%
RO ASTM RPD	228.5	−0.2%	176.0	−20.4%	148.0	−15.9%	140.0	−16.7%

Table 6 – ROPS displacement at maximum absorbed energy (C3D4).

	Allis Chalmers 5040 ROPS				Long 460 ROPS			
	Rear (mm)	Error (%)	Side (mm)	Error (%)	Rear (mm)	Error (%)	Side (mm)	Error (%)
RAD	426	–	295	–	400	–	360	–
Experimental RPD	229	0.0%	221	0.0%	176	0.0%	168	0.0%
ASTM RPD	245.0	7.0%	189.0	−14.5%	161.0	−8.5%	132.0	−21.4%
RO O'Neal steel RPD	244.0	6.6%	189.0	−14.5%	157.0	−10.8%	127.0	−24.4%
RO ASTM RPD	221.0	−3.5%	172.0	−22.2%	143.0	−18.8%	118.0	−29.8%

Harris et al., 2011; Thambiratnam et al., 2009). Results showed that the Ramberg–Osgood model with lower q factor predicts stiffer material and consequently stiffer structure compared to the Ramberg–Osgood model with high q. This means that under the same load the stiffer structure deflects less than the more flexible structure. Comparing the stress–strain relationship in Fig. 4 with the force-deflection curves in Figs. 7–10, the predicted force-deflection curves of ROPS follow the same trend as the strain–stress curves of material (Figs. 7–10).

The differences between the experimental and predicted force-deflection curves may be due to the bolt adjustments at the holes in experimental tests. The simulated structure in the FE model is a single part, which cannot predict adjustments at bolt holes. Results showed that the FE model predicted the force-deflection curves under the rear load more accurately than the side load test (Figs. 7–10). In the experimental side load test, the force was applied in a plane perpendicular to the bolt pivot joints. There may be some movement between the ROPS parts and rotation around the pins pivot point, as the ROPS was an assembled structure. The bolt adjustment and lock up in the hole may be another reason which apparently happened at 40 mm deflection in the side load test of Long 460 ROPS as seen by a sharp increase in the curve slope in Fig. 10. The FE model geometry consists of one part and could not predict any movement between parts and rotations around the pivot point. The FE model results might be improved by modelling an assembled structure rather than a fixed structure to enable the prediction of movements between parts, pin adjustments at holes, and rotations at pivot points.

The energy–deflection curve for each test was developed by calculating the area under the force-deflection curve. The energy–deflection curve for rear and side loading tests of Allis Chalmers ROPS are presented in Figs. 11 and 12. Figures 13 and 14 demonstrate the energy–deflection curves of Long 460 ROPS. The energy–deflection curves were used to calculate the RPD. In the simulated tests, the RPD is the vertical projection of the intersection point of the energy–deflection curve with the predefined level of absorbed energy. For example, the RPD for the Allis Chalmers ROPS in rear loading test with material properties based on ASTM constitutive relation with the predefined level of energy (2845 J) is 255.5 mm (Fig. 11). For ROPS to pass the standard tests, the RPD should be smaller than RAD. In all of the experimental and simulated tests RPD is much lower than the RAD (Tables 5 and 6).

While the test outcome (pass or fail) is an important output of these tests, it is also important that the developed force-deflection curves be close to the experimental test results. An accurate FE model can be used as a design tool and also as a tool to predict the effect of minor structural modifications on ROPS behaviour under the test. The error was calculated comparing the experimental RPD with the predicted RPD (Tables 5 and 6) using Eq. (5):

$$\text{Error\%} = \frac{\text{RPD}_\text{P} - \text{RPD}_\text{E}}{\text{RPD}_\text{E}} \times 100 \quad (5)$$

where RPD_P is predicted RPD and RPD_E is experimental RPD.

Both ROPS passed all of the experimental and simulated tests. Errors for three out of four virtual tests based on ASTM

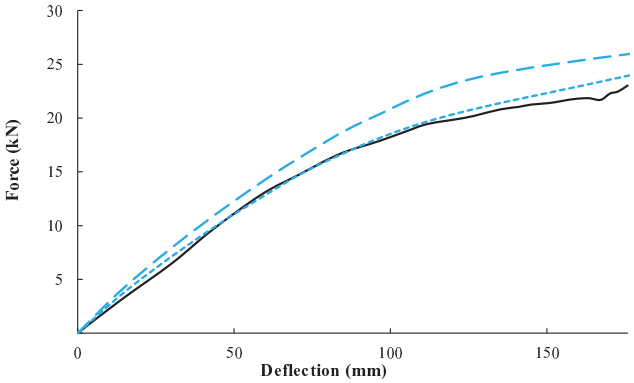

Fig. 15 – Long 460 ROPS experimental and virtual rear load test with two element types and element sizes. Experimental test results (——), FE results for the model with element type (C3D4) and global size 0.08 (— —), and FE results for the model with element type (C3D10M) and global size 0.01 (– – –).

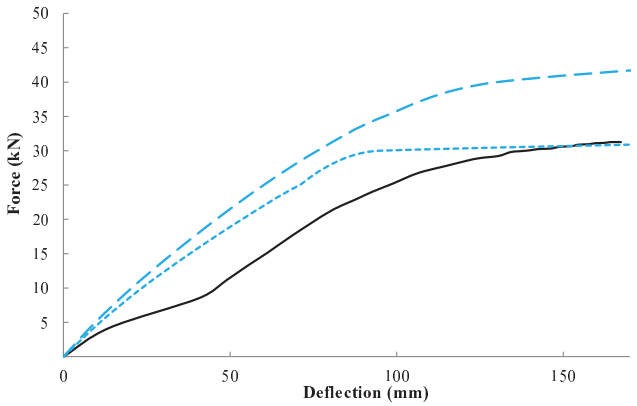

Fig. 16 – Allis Chalmers 5040 ROPS experimental and virtual side load test with two element types and element sizes. Experimental test results (——), FE results for the model with element type (C3D4) and global size 0.08 (— —), and FE results for the model with element type (C3D10M) and global size 0.01 (– – –).

material properties were smaller than the Ramberg–Osgood (RO) models. For example the average error for FE models (C3D10M) ASTM, RO O'Neal, and RO ASTM, were 9.6, 12.1, and, 13.3% respectively. The developed FE models based on ASTM predicted the shape of the experimental force-deflection curves better than the FE models developed based on the RO material model (Figs. 7–10).

Comparing the virtual test results for the meshed ROPS with C3D4 node (element size 0.08 m) and C3D10M node (element size 0.01 m), showed that the coarse linear elements were stiffer than the fine quadratic elements (Figs. 15 and 16). Both the node order and global size were effective to increase the structure flexibility. Therefore the ROPS with C3D4 elements deflects less than the ROPS with C3D10M elements. The developed FE models applying quadratic tetrahedral (C3D10M) elements predicted the ROPS behaviour under virtual tests better than developed FE models with coarse linear tetrahedral (C3D4) elements. The RPD percent errors for ROPS with C3D4 elements were higher than C3D10M elements for all of the tests except for the rear test of Allis Chalmers 5040 ROPS (Tables 5 and 6). The computational time for the model with coarse C3D4 and fine C3D10Melements were approximately 5 and 10 min for each analysis step (loading point), respectively.

4. Conclusion

Several FE models have been developed to predict the performance of the ROPS in recent years, but none of these models predict the behaviour of the ROPS designed by CRDP. The aim of this study was to develop an FE model to predict the behaviour of the ROPS designed by CRDP, under SAE J2194 standard test. Non-linear FE models were developed for rear and side load tests with variation in element type and size as well as material properties. The FE models were not calibrated. They were validated by comparing virtual test results with the experimental test results of two models of ROPS (Allis Chalmers 5040 and Long 460).

Results showed that the developed FE models can predict the rear test results more accurately than the side load test results. In most of the side tests the FE models were stiffer than the experimental tests, because the developed geometries included a single part and did not consider the adjustments at holes, rotations, and movements between parts. The developed FE model, applying experimentally measured material properties predicted the test results more accurate than FE models developed based on constitutive laws, in three out of four tests. The meshed ROPS with fine quadratic mesh (C3D10M node, global size 0.01 m), resulted in the more accurate FE model compared to the linear coarse mesh (C3D4 node, 0.08 m).

The two ROPS passed all of the virtual tests and the experimental tests. Therefore all of the finite element results appear to be acceptable. The other criterion that was considered for evaluating the FE tests reliability is the similarity of force-deflection curves of the virtual tests with the experimental tests.

The developed FE models using the ASTM material properties and meshed ROPS with C3D10M elements with global size 0.01 m are recommended for future test FE models. The average error for FE model (ASTM, C3D10M, 0.01) was less than 10% compared to experimental test measurements and the predicted force-deflection curve more closely matched the experimental force-deflection curves.

Acknowledgements

This work was supported by the United States National Institute for Occupational Safety and Health (NIOSH 5U54OH008085-12). The authors would like to acknowledge the FEMCO, Inc. for conducting the experimental tests.

REFERENCES

Alfaro, J. R., Arana, I., Arazuri, S., & Jarén, C. (2010). Assessing the safety provided by SAE J2194 Standard and Code 4 Standard code for testing ROPS, using finite element analysis. *Biosystems Engineering, 105*(2), 189–197. http://dx.doi.org/10.1016/j.biosystemseng.2009.10.007.

Ayers, P., Dickson, M., & Warner, S. (1994). Model to evaluate exposure criteria during roll-over protective structures (ROPS) testing. *Transactions of the ASAE, 37*(6), 1763–1768.

Ayers, P., Khorsandi, F., John, Y., & Whitaker, G. (2016). Development and evaluation of a computer-based ROPS design program. *Journal of Agricultural Safety and Health, 22*(4), 247–260. http://dx.doi.org/10.13031/jash.22.11745.

Bureau of Labor Statistics. (2014). *Census of fatal occupational injuries summary, 2013*. Retrieved 5 October 2015, from Bureau of Labor Statistics www.bls.gov/news.release/cfoi.nr0.htm.

CDC. (2014). *Workplace safety and health topic: 25 June 2014*. Retrieved Accessed 5 November 2014, from Center for disease control and prevention www.cdc.gov/niosh/topics/aginjury/.

Chen, C., Wang, G., Zhang, Y., Zhang, Y., & Si, J. (2012). Effect of lateral stiffness coefficient of loader ROPS on human injury in a lateral rollover incident. *Biosystems Engineering, 113*(2), 207–219.

Chisholm, C. (1979). A mathematical model of tractor overturning and impact behaviour. *Journal of Agricultural Engineering Research, 24*(4), 375–394.
Clark, B. J. (2005). *The behaviour of rollover protective structures subjected to static and dynamic loading conditions* (PhD). Queensland University of Technology (16292).
E8/E8M-11. (2011). *Standard test methods for tension testing of metallic materials*.
EEC. (1987). *Roll-over protection structures mounted in front of the driver's seat on narrow-track wheeled agricultural and forestry tractors European Economic Community, Directive 87/402/EEC*. Strasbourg.
Ellobody, E. (2014). *Finite element analysis and design of steel and steel–concrete composite bridges*. Butterworth-Heinemann.
Fabbri, A., & Ward, S. (2002). PM—Power and machinery: Validation of a finite element program for the design of Roll-over Protective Framed Structures (ROPS) for agricultural tractors. *Biosystems Engineering, 81*(3), 287–296. http://dx.doi.org/10.1006/bioe.2001.0012.
Harris, J., Mucino, V., Etherton, J., Snyder, K., & Means, K. (2000). Finite element modeling of ROPS in static testing and rear overturns. *Journal of Agricultural Safety and Health, 6*(3), 215–225.
Harris, J., Winn, G., Ayers, P., & McKenzie, E., Jr. (2011). Predicting the performance of cost-effective rollover protective structure designs. *Safety Science, 49*(8), 1252–1261.
Hoy, R. M. (2009). Farm tractor rollover protection: Why simply getting rollover protective structures installed on all tractors is not sufficient. *Journal of Agricultural Safety and Health, 15*(1), 3–4.
Karliński, J., Rusiński, E., & Smolnicki, T. (2008). Protective structures for construction and mining machine operators. *Automation in Construction, 17*(3), 232–244.
Kim, T., & Reid, S. (2001). Multiaxial softening hinge model for tubular vehicle roll-over protective structures. *International Journal of Mechanical Sciences, 43*(9), 2147–2170.
Mangado, J., Arana, I., Jarén, C., Arnal, P., Arazuri, S., & de León, J. P. (2007). Development and validation of a computer program to design and calculate ROPS. *Journal of Agricultural Safety and Health, 13*(1), 65–82.
Murphy, D. J., & Buckmaster, D. R. (2014). *Rollover protection for farm tractor operators*. Retrieved 9 March 2015 http://extension.psu.edu/business/ag-safety/vehicles-and-machinery/tractor-safety/e42.
Murphy, D. J., & Yoder, A. (1998). Census of fatal occupational injury in the agriculture, forestry, and fishing industry. *Journal of Agricultural Safety and Health, 4*(5), 55.
OECD. (2008). *OECD standard code for the official testing of rollover protective structures on agricultural and forestry tractors. Organization for the Economic Co-operation and Development*. Paris: France.
OECD. (2012). *CODE 4. OECD standard code for the official testing of protective structures on agricultural and forestry tractors (static test)*.
OEEC. (1959). *OEEC standard code for the official testing of agricultural and forestry tractors*. Paris, France: Organization for the European Economic Co-operation.
Rasmussen, K. J. (2003). Full-range stress–strain curves for stainless steel alloys. *Journal of Constructional Steel Research, 59*(1), 47–61.
Reynolds, S. J., & Groves, W. (2000). Effectiveness of roll-over protective structures in reducing farm tractor fatalities. *American Journal of Preventive Medicine, 18*(4), 63–69.
Ross, B., & DiMartino, M. (1982). Rollover protective structures. Their history and development. *Professional Safety, 27*, 15–23.
SAE. (2009). *Roll-Over Protective Structures (ROPS) for wheeled agricultural tractors. SAE J2194*. SAE International.
Springfeldt, B. (1996). Rollover of tractors—international experiences. *Safety Science, 24*(2), 95–110.
Swan, S. A. (1988). *Rollover protective structure (ROPS) performance criteria for large mobile mining equipment. Information Circular/1988 (PB-90–265448/XAB; BUMINES-IC–9209)*. Retrieved from United States: https://www.osti.gov/scitech/biblio/6777991.
Thambiratnam, D. P., Clark, B. J., & Perera, N. (2009). Performance of a rollover protective structure for a bulldozer. *Journal of Engineering Mechanics, 135*(1), 31–40.
Thelin, A. (1998). Rollover fatalities—Nordic perspectives. *Journal of Agricultural Safety and Health, 4*(3), 157.
Wei, D., & Elgindi, M. B. (2013). Finite element analysis of the Ramberg-Osgood bar. *American Journal of Computational Mathematics, 3*(03), 211.
Yeh, R. E., Huang, Y., & Johnson, E. L. (1976). *An analytical procedure for the support of ROPS design. SAE Technical Paper (760690)*. Retrieved from http://papers.sae.org/760690/.
Yu, M.-H., & Li, J.-C. (2012). *Computational plasticity: With emphasis on the application of the unified strength theory*. Springer Science & Business Media.